ELSEVIER

Marine Chemistry 69 (2000) 139–152

MARINE CHEMISTRY

www.elsevier.nl/locate/marchem

Photogeneration of singlet oxygen and free radicals in dissolved organic matter isolated from the Mississippi and Atchafalaya River plumes

Sonya L. Holder Sandvik [a,b,*], Piotr Bilski [b], J. Dean Pakulski [a,1], Colin F. Chignell [b], Richard B. Coffin [c]

[a] *National Research Council Fellow, U.S. Environmental Protection Agency, Gulf Breeze, FL 32561, USA*

[b] *Laboratory of Pharmacology and Chemistry, National Institute of Environmental Health Sciences, National Institutes of Health, Research Triangle Park, NC 27709, USA*

[c] *Naval Research Laboratory, EQSS, Code 6115, 4555 Overlook Dr., Washington, DC 20375, USA*

Received 22 March 1999; accepted 19 October 1999

Abstract

The photoreactivity to UV light of ultrafiltered dissolved organic matter (DOM) collected during cruises along salinity transects in the Mississippi and Atchafalaya River plumes was examined by measuring photogenerated free radicals and singlet molecular oxygen ($^1O_2$) photosensitization. Singlet oxygen was detected by its infrared phosphorescence at 1270 nm using both steady-state and time-resolved techniques. The $^1O_2$ quantum yields were corrected for self-quenching of $^1O_2$ by the DOM substrates. Photogenerated free radicals were monitored by electron paramagnetic resonance (EPR). Two size fractions of the dissolved organic matter were examined: material retained with a 3 kDa cut-off filter and material retained with a 1 kDa cut-off filter. The highest $^1O_2$ quantum yields were found in the lower molecular mass material. There was little change in the $^1O_2$ quantum yields with increasing salinity, indicating that the photosensitizing ability of the estuarine DOM does not decrease as terrestrial DOM is transported to sea and mixes with marine DOM. In contrast to $^1O_2$ formation, the steady-state levels of photoproduced free radicals did not significantly differ between high and low molecular mass DOM, and the levels were substantially higher in riverine DOM than along plume salinity transects. This rapid transition in free radical level suggests that terrestrially-derived DOM experiences significant changes in this aspect of its photoreactivity in low (< 10 ppt) salinity waters. Published by Elsevier Science B.V.

Keywords: dissolved organic matter; singlet oxygen; EPR; ultrafiltration; photochemistry; coastal waters

1. Introduction

In natural waters, nutrient and carbon cycling is driven in part by solar ultraviolet (UV) excitation of

* Corresponding author. Laboratory of Pharmacology and Chemistry, National Institute of Environmental Health Sciences, National Institutes of Health, MD F0-06, P.O. Box 12233, Research Triangle Park, NC 27709, USA. Tel.: +1-919-541-5768; Fax: +1-919-541-1043; E-mail: sandvik@niehs.nih.gov

[1] Present address: Ocean Sciences Centre, Memorial University of Newfoundland, St. John's, NF, Canada, A1C 5S7.

0304-4203/00/$ - see front matter Published by Elsevier Science B.V.
PII: S0304-4203(99)00101-2

chromophoric dissolved organic matter (CDOM) (Stumm and Morgan, 1996; Moran and Zepp, 1997). Direct photolysis and mineralization of CDOM has been observed by measuring the release of dissolved inorganic carbon (Miller and Zepp, 1995). Irradiation of CDOM also enhances bacterial growth, indicating that the material can be degraded into more labile material for microbial utilization (Kieber et al., 1990; Wetzel et al., 1995; Miller and Moran, 1997; Bertilsson and Tranvik, 1998). Monitoring the photoreactivity of CDOM may thus enhance our knowledge of the role and fate of these substances in aquatic systems.

The photoreactivity of CDOM depends on its chemical composition, which is determined mainly by its origin. Terrigenous dissolved organic matter, found in lakes and rivers, is characterized by higher carbon to nitrogen ratios and is enriched in aromatic compounds relative to material of marine origin (Benner et al., 1992; Hedges et al., 1992). Marine organic matter, thought to form de novo in seawater (Carder et al., 1989; Coble et al., 1998), has been shown to be optically distinct by fluorescence spectroscopy (Coble and Brophy, 1994; Coble, 1996). Differences in chemical composition may influence the photochemistry of CDOM in estuarine environments as dissolved organic matter (DOM) of terrestrial origin is mixed with marine DOM along estuarine salinity gradients.

A number of studies on the distribution of DOM in nearshore systems indicate removal and/or conservative dilution of terrigenous DOM (Mantoura and Woodward, 1983; Benner et al., 1992; Guo et al., 1995). Other investigations, however, focus on photochemical and microbial transformations of terrigenous DOM, which may contribute to the productivity in these nearshore systems (Moran et al., 1991; Chin-Leo and Benner, 1992; Bushaw et al., 1996; Opsahl and Benner, 1997). Optical absorption and fluorescence of CDOM also vary across estuarine salinity gradients, indicating photobleaching and removal/dilution of terrigenous CDOM (Blough et al., 1993; Vodacek et al., 1997). These changes in the optical absorption and fluorescence characteristics of bulk CDOM may reflect changes in the photoreactivity resulting from the mixing and transformation of terrigenous and marine CDOM in low salinity environments.

At present, the chemical and structural transformations of CDOM following UV irradiation are not fully understood. CDOM strongly absorbs UV light and can act as a photosensitizer and as a reaction substrate, leading to the production of numerous transient intermediates and terminal photoproducts (Cooper et al., 1989; Blough and Zepp, 1995; Blough, 1997). A number of these intermediates are highly reactive oxygen species, such as singlet molecular oxygen, which has been observed in solutions of humic and fulvic acids and in natural waters (Zepp et al., 1985; Haag and Hoigné, 1986). Photoirradiation of CDOM also leads to photoionization (Fischer et al., 1985) and formation of free radicals, some of which have been identified, such as the hydroxyl radical ($^{\cdot}OH$) (Zafiriou, 1974; Mopper and Zhou, 1990; Vaughan and Blough, 1998), superoxide anion radical ($O_2^{\cdot -}$) (Petasne and Zika, 1987; Zafiriou, 1990), and peroxy radicals ($ROO^{\cdot}$) (Faust and Hoigné, 1987; Blough, 1988; Kieber and Blough, 1990).

Formation of free radicals and reactive oxygen species can lead to chemical transformations of compounds. Singlet molecular oxygen ($^1O_2$), is a short-lived, and highly reactive intermediate that may be important in the formation of secondary (photo)products under some conditions. It is formed by quenching CDOM excited triplet-states, and is therefore one indicator of the photosensitizing ability of the CDOM. Free radicals are formed during direct photolysis of the CDOM and can be detected by electron paramagnetic resonance (EPR). Radical reactions can lead to the degradation of molecules into smaller photoproducts as well as to the combination of radicals and substrates into larger molecular compounds, thereby influencing chemical and microbial activity in natural waters.

In the present investigation, we characterized the photoreactivity of CDOM isolated from freshwater, estuarine and coastal waters by measurement of singlet oxygen production and free radicals upon exposure to UV light. The CDOM was isolated from the Apalachicola, Atchafalaya, Blackwater and Mississippi River systems discharging into the Gulf of Mexico. In the Mississippi and Atchafalaya River plumes, we followed a salinity gradient into the Gulf of Mexico to track the change in photoreactivity of CDOM going from riverine to coastal waters.

2. Material and methods

2.1. Sample sites and collection

Surface water from the Mississippi and Atchafalaya River plumes was collected in June 1995 and February 1996 during two OSV *Anderson* cruises along salinity transects originating in the rivers and extending into the Gulf of Mexico. The Atchafalaya River originates at the confluence of the Mississippi and Red rivers via a diversion channel at Simmsport, Louisiana and discharges into Atchafalaya Bay, located to the west of the Mississippi delta. The Atchafalaya interacts with extensive areas of wetlands below the Simmesport junction. In contrast, the Mississippi River below this junction is highly channeled and has little interaction with its historical flood plains. Samples were also collected from the Apalachicola River in Apalachicola, Florida in May 1995 and the Blackwater River in Milton, Florida in February 1996. The Apalachicola watershed drains the piedmont region of Georgia and Alabama. The Blackwater is a small coastal river originating in Northeast Florida and is characterized by high concentrations of humic material. For comparison, a soil-derived humic acid purchased from Aldrich Chemical was also examined.

Sample water was collected with a teflon lined submersible pump (<1.0 m below surface) into clean (10% HCl and MilliQ water rinsed) 50 l polyethylene carboys prior to ultrafiltration. Initial sample volume ranged from 40 l in the rivers to 150 l at the high salinity coastal stations. The water was prefiltered using a 10 μm Nucleopore polycarbonate cartridge filter followed by a 0.2 μm Nucleopore polycarbonate cartridge filter. Samples were concentrated by tangential-flow ultrafiltration using a 3 kDa polysulfone Amicon filter. Filter cartridges were cleaned with 0.1 N NaOH and rinsed with MilliQ water. Between samples, filters were flushed with 0.01 N NaOH followed by a MilliQ water rinse. In the field, samples were concentrated to an approximate volume of 250 ml, collected into HCl/MilliQ rinsed Nalgene bottles and frozen at -20°C. In the laboratory, the concentrate was lyophilized to a dry solid state. Throughout this report these >3 kDa samples will be referred to as high molecular mass (HMM) samples.

Two additional samples of Mississippi River and Gulf of Mexico DOM were obtained from R. Benner (Marine Sciences Institute, University of Texas at Austin, Port Aransas, TX). These latter samples, with initial volume ranging from 100 to 200 l of 0.2 μm filtered water, were concentrated using an Amicon DC-10 ultrafiltration system equipped with 1 kDa cut-off polysulfone filters. The >1 kDa, Gulf of Mexico sample concentrate was diafiltered with 18 l of Milli-Q water to remove salts and dried using a Savant Speed Vac system. In this report, these >1 kDa inclusive samples will be referred to as low molecular mass (LMM) samples.

After lyophilization, the dry solids were dissolved in D_2O (deuterium oxide, 99.9%, Cambridge Isotope Laboratories) for the singlet oxygen experiments and in either D_2O or deionized water for the EPR experiments.

In addition, 50 ml samples of the initial 0.2 μm filtered water and the ultrafiltration permeate water were collected for optical absorption analysis. These samples were stored in foil covered sterile polyethylene centrifuge tubes at -20 EC. Prior to the cruises, preliminary experiments found no change in the absorption spectra for similar samples stored in this manner for seven weeks.

2.2. Optical absorption measurements

Absorption spectra were measured with a Hewlett-Packard 8452 diode array spectrophotometer with MilliQ filtered water as a reference. A 10 cm path length quartz cell was used for the initial and permeate samples and a 1 cm quartz cell was used for the concentrated samples. Before measurement, samples were warmed to room temperature and thoroughly mixed.

In agreement with observations by other researchers, the spectra exhibited a general exponential behavior across the visible region (Bricaud et al., 1981; Zepp and Schlotzhauer, 1981; Davies-Colley and Vant, 1987; Blough et al., 1993). In most of the spectra a shoulder was observed at 265 nm, which has been assigned to small organic molecules such as purine and pyrimidine (Yentsch and Reichert, 1962). In some samples a peak was also observed at 360 nm. This second peak was only significant in two samples (T1A and T1B, Table 1) in the June

Table 1
Values of S for initial water (0.2 μm filtered) collected along two salinity transects

River system	Sample	Location	Salinity (ppt)	S (nm^{-1})
June 1995				
Atchafalaya	T1A	28°00′N, 90°06′W	28	0.0191
Atchafalaya	T1B	29°02′N, 91°40′W	15	0.0170
Atchafalaya	T1D	29°07′N, 91°32′W	9	0.0177
Atchafalaya	T1E		0	0.0175
Mississippi	T2C	28°39′N, 89°38′W	30	0.0169
Mississippi	T2D	28°51′N, 89°30′W	5	0.0172
Mississippi	T2E	29°12′N, 89°18′W	0	0.0169
February 1996				
Mississippi	MD	28°41′N, 89°30′W	27	0.0176
Mississippi	MC	28°49′N, 89°29′W	16	0.0177
Mississippi	MB	28°53′N, 89°27′W	30	0.0179
Mississippi	MA	29°12′N, 89°17′W	0	0.0159
Atchafalaya	AD	28°57′N, 91°43′W	28	0.0176
Atchafalaya	AC	29°11′N, 91°35′W	24	0.0173
Atchafalaya	AB	29°12′N, 91°32′W	12	0.0168
Atchafalaya	AA	29°15′N, 91°30′W	0	0.0165

Atchafalya transect. For our analysis of the 0.2 μm-filtered water samples before concentration, the relatively narrow peak ($width_{1/2\ max} \sim 35$ nm) was subtracted from the exponential curve of the CDOM absorption. The 360 nm peak was not present in the concentrate after ultrafiltration for either of these samples.

The apparent absorption coefficient α_λ for all samples was determined from

$$\alpha_\lambda = 2.303\,A(\lambda)/l \quad (1)$$

for wavelength λ in nm, where l is the optical path length of the cell in meters and $A(\lambda)$ is the baseline corrected absorbance. The baseline correction consisted of subtracting an average of the absorbance between 750 nm and 800 nm from each spectrum. Most of the spectra could then be fit with a simple exponential decay,

$$\alpha_\lambda = \alpha_r e^{S(r-\lambda)} \quad (2)$$

where α_r is the apparent absorption at a reference wavelength r, and the fitting parameter, S, can be used to compare samples. Carder et al. (1989) reported that S depends on the chosen wavelength range. In our data, we saw a similar small reduction in S when including the longer wavelengths. For example, evaluating S for sample T1D for different wavelength ranges gives $S_{290-608} = (16.67 \pm 0.09) \times 10^{-3}$ nm^{-1}, $S_{290-500} = (17.28 \pm 0.07) \times 10^{-3}$ nm^{-1}, and $S_{290-450} = (17.70 \pm 0.06) \times 10^{-3}$ nm^{-1}, where the reported error is from a calculated least-squares fit to the natural logarithm linearized absorption. For consistency and because there is more error associated with including the absorption at longer wavelengths, all S values were evaluated for the 290 to 450 nm region.

2.3. Singlet oxygen lifetime and quantum yield measurements

The singlet oxygen quantum yield, ϕ_{so}, in our samples was determined by direct measurement of the singlet oxygen phosphorescence at 1200–1350 nm in steady-state experiments. In H_2O, the lifetime, τ_{so}, of singlet oxygen is very short (~ 4 μs), making the phosphorescence intensity very weak and difficult to observe. To increase the lifetime, and thereby the intensity of the steady-state signal, dry solids lyophilized from the concentrate were dissolved in D_2O, in which the $^1O_2$ lifetime is about 10 times longer (Bilski et al., 1997). Excitation light was provided by a 250 Watt medium pressure mercury lamp (Kratos) and was filtered to only allow wavelengths in the 280–380 nm range. The relative intensities of the main emission lines in this wavelength region are similar to those given by Gould (1989) for medium pressure mercury arc lamps. The phosphorescence was measured by a germanium diode detector cooled to 77 K. Signal to noise ratio was increased by using an optical chopper coupled to a lock-in amplifier. Air was bubbled through the samples during measurement to ensure mixing and a constant oxygen concentration. The quantum yield was calculated using perinaphthenone (Aldrich Chemical), with $\phi_{so} \approx 1$, as a standard (Schmidt et al., 1994).

Immediately before irradiating the sample to generate $^1O_2$ phosphorescence, the absorption of the CDOM dissolved in D_2O was measured with a Hewlett-Packard 8452 diode array spectrophotometer using the same 1 cm path length quartz cell for both the absorption measurement and for $^1O_2$ excitation. Absorption spectra were also recorded for any optical filters used in the excitation beam line. The

absorbance was first normalized for zero absorption above 750 nm and the slope of the log-linearized absorption was compared with that found for the absorption of the sample before concentration. In order to calculate the singlet oxygen quantum yields, the integrated absorption, N, was determined by

$$N = \int_{250}^{450} \left[\left(1 - 10^{-A(\lambda)}\right) \times \left(\prod_i F_i(\lambda)\right) \times \text{L.R.}(\lambda) \right] \mathrm{d}\lambda \quad (3)$$

where $A(\lambda)$ is the measured absorbance, F_i (λ) is the percent transmittance spectra of each filter used in the incident beam line, and the lamp response, L.R.(λ), is the calibrated number of photons emitted by the lamp at each wavelength.

Singlet oxygen lifetimes were measured using a optical system employing a pulsed laser (Photonics MY-33 Nd:YAG) and a germanium diode detector coupled to a HP 54111D digitizing oscilloscope. A detailed description of the pulsed spectrometer has been published elsewhere (Bilski and Chignell, 1996). Perinaphthenone was added to the CDOM solutions as an efficient sensitizer. Changes in sample τ_{so} from that of a perinaphthenone control solution indicated quenching of the singlet oxygen by the CDOM substrate. The τ_{so} of each sample was measured and used to correct the ϕ_{so}'s determined in the steady-state experiment. For a few representative samples, τ_{so} was measured as a function of CDOM concentration.

To calculate ϕ_{so}, the ratio of the emitted quanta of light to the absorbed quanta of light was determined and normalized to a standard, in this case perinaphthenone (with a ϕ_{so} of unity), as follows:

$$\phi_{so} = \frac{h_{CDOM} \times \dfrac{\tau_{so,\,standard}}{\tau_{so,\,CDOM}} \times N_{standard}}{N_{CDOM} \times h_{standard}} \quad (4)$$

where h is the height of the singlet oxygen phosphorescence peak, and N was calculated from Eq. (3). The experimental uncertainty values we report for the singlet oxygen quantum yields in Table 2 are calculated from the signal-to-noise ratio of the measured phosphorescence curve for a single sample and are not statistical uncertainties found from the measurement of multiple samples from each location.

2.4. EPR detection of free radicals

EPR spectra were recorded with a Varian E-line Century Series X-band spectrometer using a TE_{102} cavity with a window for irradiation. The light source was a 350 W high pressure mercury lamp (Oriel) with a distilled water filter in the beam-line to reduce heating of the sample. Since no optical filters were used, all emission lines of the lamp, including short

Table 2
Singlet oxygen quantum yields. The listed salinity is that for the initial water sample measured in the field. Size fraction refers to the nominal pore size of the cut-off filter used for ultrafiltration. The reported error is calculated from the signal to noise ratio of the $^1O_2$ phosphorescence for a single sample

	Sample	Size fraction (Da)	Salinity (ppt)	ϕ_{so}
Mississippi (1995)	T2C	> 3000	30	0.017 ± 0.005
Mississippi (1995)	T2D	> 3000	5	0.017 ± 0.004
Mississippi (1995)	T2E	> 3000	0	0.017 ± 0.001
Atchafalaya (1995)	T1A	> 3000	28	0.027 ± 0.011
Atchafalaya (1995)	T1B	> 3000	15	0.019 ± 0.003
Atchafalaya (1995)	T1D	> 3000	9	0.020 ± 0.001
Atchafalaya (1995)	T1E	> 3000	0	0.016 ± 0.001
Gulf of Mexico	BGOM	> 1000	34 to 36	0.039 ± 0.001
Mississippi River	BMISS	> 1000	0	0.061 ± 0.001
Apalachicola River	APP	> 3000	0	0.014 ± 0.001
Aldrich Humic Acids	ALD	unknown	0	0.010 ± 0.002
Mississippi (1996)	MD	> 3000	27	0.020 ± 0.003
Mississippi (1996)	MC	> 3000	16	0.018 ± 0.002
Mississippi (1996)	MA	> 3000	0	0.017 ± 0.001
Blackwater River	BWR	unknown	0	0.038 ± 0.001

wavelength lines in the UVC region (190–290 nm), were allowed to reach the sample. A suprasil flat cell (Wilmad) was used to insure transparency in the UV region. Typical parameter settings were: power, 20 mW; modulation amplitude, 1 G; time constant, 1 s; modulation frequency, 100 kHz; scan range, 100 G. All scans were made at room temperature. We found the EPR signal strength in the CDOM samples to be optimized at pH = 10.8. All samples were buffered to this pH using a 0.25 M Na_2HPO_4 solution, which has no significant absorption in the UV region. The enhancement of the EPR signal at alkaline pH has been reported for aqueous solutions of humic and fulvic acids (Haworth, 1971; Senesi and Schnitzer, 1977), and was suggested to be due to increased stabilization of substituted semiquinone radicals as semiquinone ions (Senesi and Schnitzer, 1977).

About 0.7 ml of the sample (dry solid dissolved in deionized H_2O) was placed in the EPR flat cell, which had a 0.3 mm optical path length. Absorption spectra were recorded immediately prior to EPR measurements to later normalize the EPR results for concentration differences between the samples.

Dark control scans were taken immediately before illumination with identical parameters to the irradiated scans. Exposure time (total exposure time < 3 min) was shutter-controlled so that scans were taken after the same UV dosage. The only parameter change between various samples was a change in the receiver gain between the strongly absorbing and the weakly absorbing samples.

The EPR signal for the solvated samples consisted of a single resonance line. In order to calculate a number representing the amount of free radicals, the peak-to-peak amplitude of the signal was measured and adjusted for the different gain settings. As an estimate of the integrated UV absorption, the baseline-corrected absorbance was integrated from 250 to 700 nm. This value was used to normalize for concentration differences between samples. We then defined a quantity called the free radical product, F.R.P., the absorption normalized, steady-state level of photoproduced free radicals accumulated under the above experimental conditions, to be

$$\text{F.R.P.} = \frac{Y_{\text{p-p}}}{\int_{250\,\text{nm}}^{700\,\text{nm}} A(\lambda)\,\mathrm{d}\lambda} \qquad (5)$$

where $Y_{\text{p-p}}$ is the gain corrected, peak-to-peak EPR signal amplitude.

Lacking a measured spectral response of the lamp used for excitation, the calculated F.R.P. is a relative yield which cannot be directly compared to results reported by other researchers. Therefore, for the EPR experiments, we compare results only within this study.

3. Results

3.1. Optical absorption

To obtain a preliminary description of the CDOM before the ultrafiltration procedure, we measured the optical absorption of the initial (0.2 μm filtered) water. In both June and February, the optical absorption parameter *S* varied slightly along the salinity transects, with a small tendency to increase as the salinity approached 30 ppt (Table 1). Small changes were also seen in the zero salinity samples, with the February samples giving a slightly lower *S*. Our values fell within the range of 0.0159–0.0191 nm^{-1}, with a mean of 0.0173 ± 0.0007 nm^{-1}. These values are consistent with those reported for coastal waters by other studies (Blough et al., 1993; Green and Blough, 1994; Vodacek et al., 1997) which used similar wavelength regions in determination of *S*.

To monitor the possible impact of sample processing on the optical nature of the material, we compared the optical absorption of the initial water, of the permeate, of the concentrate before lyophilization, and of solutions made with the lyophilized concentrate of the June samples (Fig. 1). We found that concentrating the CDOM by the ultrafiltration procedure noticeably changed the optical absorption parameter *S*. The *S* of the concentrated material before lyophilization, as well as the *S* of the dried concentrate, dissolved in either D_2O or H_2O, was smaller than *S* of the initial samples, indicating an increase in the ratio of longer wavelength absorption to shorter wavelength absorption.

3.2. Singlet oxygen production

The photosensitizing potential, or the ability of CDOM to form photoexcited triplet states, can be

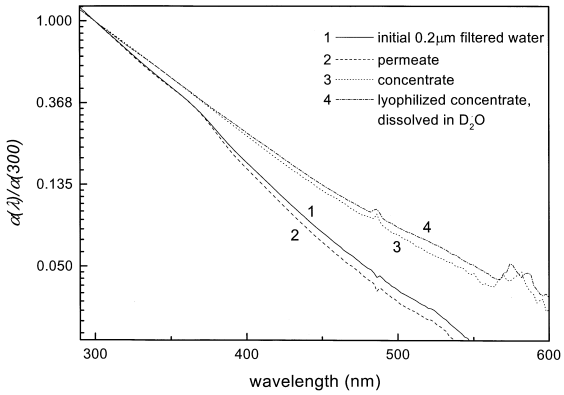

Fig. 1. Logarithmic plot of the optical absorption spectra for a zero salinity Atchafalaya River sample at different points in the ultrafiltration process. Reference wavelength chosen at 300 nm (Eq. (2)).

approximated by measuring the quantum yield of $^1O_2$ formation. For most of our samples, the $^1O_2$ phosphorescence could be observed directly in a single scan (Fig. 2). Calculation of the $^1O_2$ quantum yields of samples from different sources gave values ranging from $\phi_{so} = 0.01$ to $\phi_{so} = 0.061$ (Table 2).

The $^1O_2$ quantum yields of the LMM material are higher than those of the HMM material. For example, values for the offshore samples of the two size fractions were $\phi_{so,\,LMM} = 0.039$ and $\bar{\phi}_{so,HMM} = 0.021$ (average value for the three ≥ 27 ppt HMM samples). There was a greater difference with the inshore samples, with zero-salinity samples from the Mississippi River giving $\phi_{so,\,LMM} = 0.061$ and $\phi_{so,\,HMM} = 0.017$. The Blackwater River (BWR) lyophilized solid would only partially dissolve in D_2O at neutral pH. Because this soluble portion of the BWR sample is of unknown molecular mass and chemical composition, we cannot compare it as a HMM sample in our analysis. The size fraction of the Aldrich humic acid sample is also unknown.

Along the Mississippi River salinity transects, there was little change in the quantum yield of the HMM samples (Fig. 3). There was close agreement between summer (June 1995) and winter (February

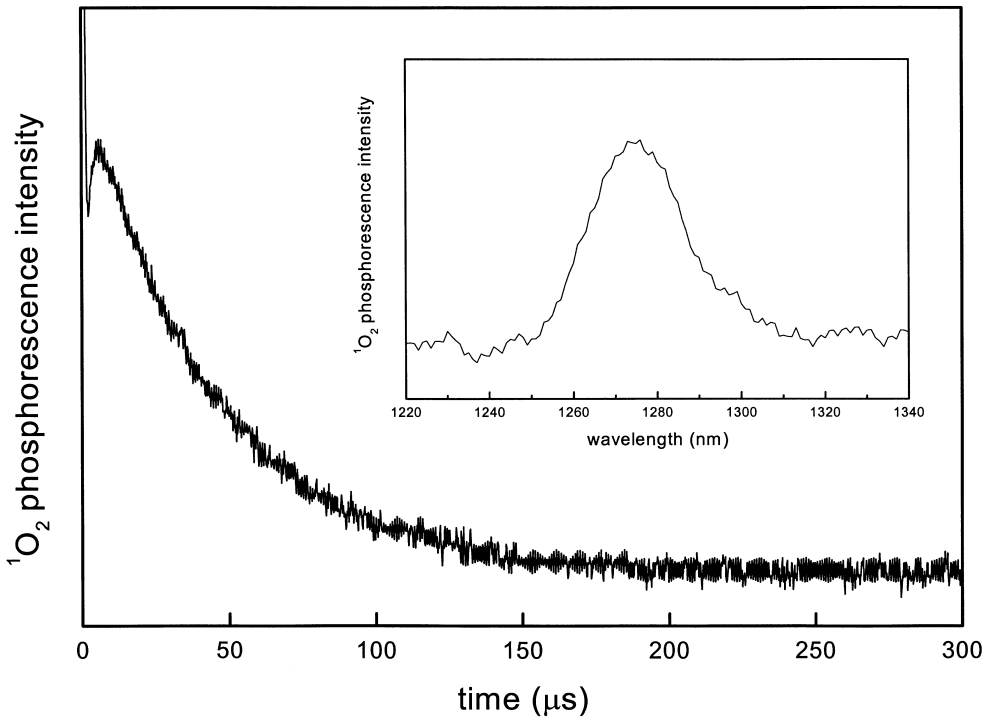

Fig. 2. Singlet oxygen phosphorescence lifetime decay for the Gulf of Mexico LMM sample dissolved in D_2O. Inset: Steady-state $^1O_2$ phosphorescence spectrum for the same sample.

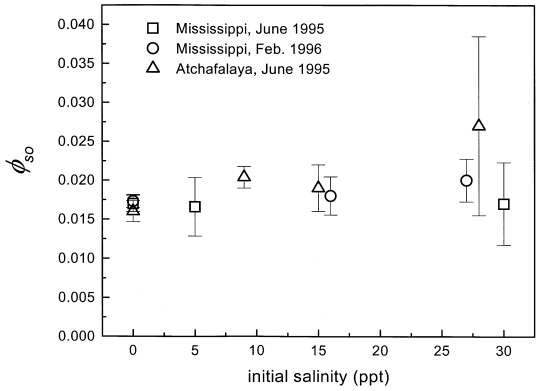

Fig. 3. ϕ_{so} values for the high molecular weight faction (HMM) CDOM samples collected from stations at different salinities along the Mississippi and Atchafalaya River transects. The error bars are calculated from the signal to noise ratio of the $^1O_2$ phosphorescence signal.

1996), but with the winter values showing a very small increase with increasing salinity. In the Atchafalaya transect, the ϕ_{so} for the inshore sample was $\phi_{so} = 0.016$, very close to the Mississippi River values, and there was a slight tendency for ϕ_{so} to increase with increasing salinity.

The soluble fraction of the Blackwater River sample gave a high value, $\phi_{so} = 0.038$. Because of the low solubility and unknown molecular mass, this value cannot be considered representative of the total collected material or of the CDOM in the river. It is interesting that this partial fraction gave such a high yield, similar to that found for the LMM samples (Table 2). In contrast, zero-salinity water from the Apalachicola River gave a low yield, $\phi_{so} = 0.014$, closer to the zero salinity values for the HMM Mississippi and Atchafalya samples.

The lowest quantum yield was found for the Aldrich humic acid sample. This low yield suggests that soil derived commercial humic acids may be less photoreactive than CDOM from natural waters.

3.3. Singlet oxygen quenching

CDOM may quench as well as produce $^1O_2$. The reduction of $^1O_2$ lifetime in the CDOM solutions, when compared to standard solution without CDOM, is an indicator of such quenching. The lifetime for singlet oxygen without CDOM was ca. $\tau_{so} = 64$ μs and was quenched to as short as ca. $\tau_{so} = 43$ μs for some of the CDOM samples in the quantum yield measurements. We then measured $^1O_2$ lifetime as a function of CDOM concentration for two samples, a zero salinity Mississippi sample (HMM) and the LMM Gulf of Mexico sample. For the Mississippi River sample, the inverse lifetime increased linearly with increasing CDOM concentration (Fig. 4), demonstrating that the CDOM quenched $^1O_2$ directly. There was a similar increase for the LMM Gulf of Mexico sample (data not shown), although the linear dependence was not as strong at low concentrations.

3.4. EPR detected free radicals

UV radiation carries enough energy to break chemical bonds in DOM to form free radicals and/or to initiate DOM photoionization, which we investigated using EPR spectroscopy.

The EPR control scans of the solutions before irradiation exhibited no signal in any case. Upon strong UV irradiation a single line EPR signal was detected with a spectroscopic g factor near $g = 2$, typical of organic radicals, and with a peak-to-peak linewidth of about 12 G (Fig. 5). There were no discernible hyperfine splittings observed in the spectrum. The signal disappeared (except for a very small, longer-lived residual) immediately upon cessation of illumination. If the irradiation continued past

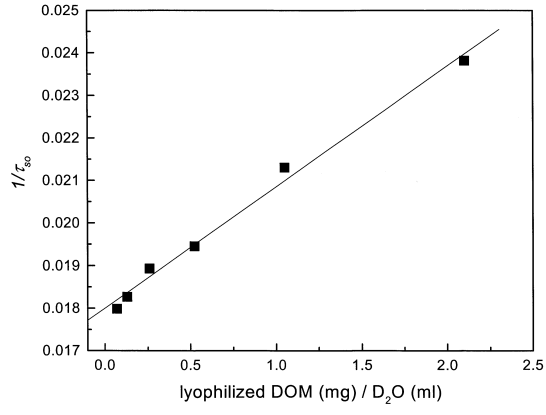

Fig. 4. $^1O_2$ quenching by CDOM for a zero salinity HMM Mississippi River sample: decreasing lifetime, τ_{so}, with increasing concentration of substrate (ultrafiltered CDOM).

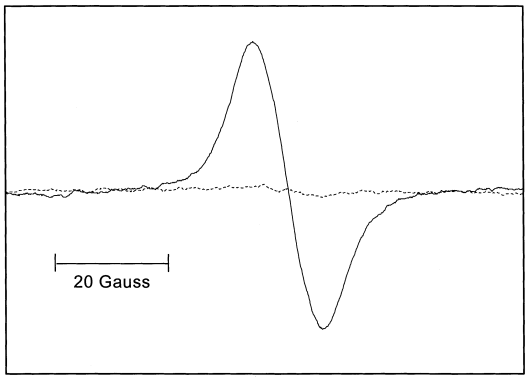

Fig. 5. Typical EPR spectrum of the steady-state, UV produced free radicals (solid line), here shown for sample MA. There was no signal in the dark control scan (dashed line) before the CDOM sample was exposed to the UV.

10 min, the signal began to decay (Fig. 6) and was not recoverable after samples were placed in the dark.

Following the treatment outlined in Section 2.4, we compared calculated free radical product (F.R.P.) values found for the HMM material and the LMM samples. The values from the LMM samples fall within the range of the HMM samples taken from the same regions (Fig. 7).

F.R.P. values were significantly higher for zero salinity CDOM than for CDOM collected from low salinity sites (Fig. 7). The F.R.P. values for the Blackwater and Apalachicola Rivers were similar to F.R.P. values for CDOM collected from zero salinity

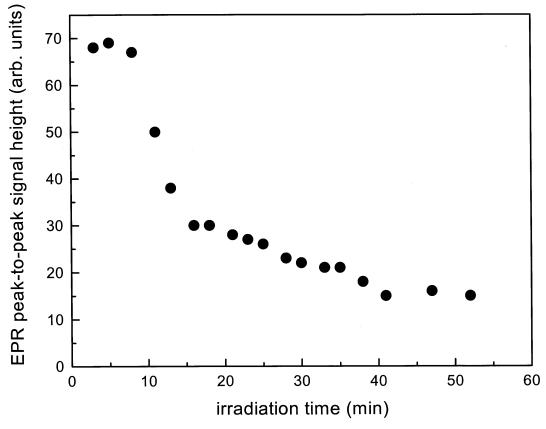

Fig. 6. Destruction of the EPR signal with continued irradiation.

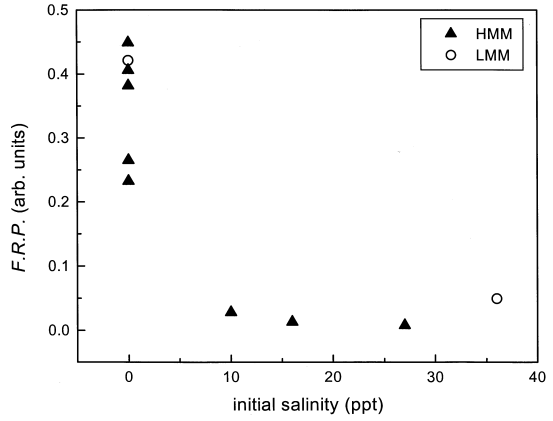

Fig. 7. The steady-state level of photoproduced free radicals, F.R.P., found for CDOM collected from stations at different salinities along the river transects. The data points correspond to the samples as follows: at zero salinity and in descending order of F.R.P. magnitude, T2E, BMISS, APP, T1E, MA, BWR; at salinity 9 ppt, T1D; at 16 ppt, MC; at 27 ppt, MD; and from 34 to 36 ppt waters, BGOM.

sites in the Mississippi and Atchafalaya Rivers (the Blackwater River sample, which did not readily dissolve in D_2O at neutral pH, was easily dissolved into alkaline solution for the F.R.P. measurement). These freshwater samples ranged from F.R.P. = 0.232 to F.R.P. = 0.448. Aldrich humic acid fell within this range with a F.R.P. = 0.318. Much lower values were seen when the salinity of the collection site increased, with F.R.P. levels ranging from 0.008 to 0.049 for sites with salinities ≥ 9. In the ϕ_{so} determination, we accounted for the presence of salts by including a correction based on the lifetime of the phosphorescence. In the EPR experiments we do not have a similar correction. However, we did not expect the salts to contribute to the observed signal, and the much higher F.R.P. value for the inshore samples versus the offshore samples holds true for both the >3 kDa cut-off material, which had not been desalted, and the >1 kDa, which had been desalted, indicating that presence of the salt plays no significant role in F.R.P.

4. Discussion

CDOM acts as a $^1O_2$ photosensitizer when longer-lived, excited triplet state(s) ($^3CDOM*$) are

formed in the light-exposed CDOM in the presence of oxygen (Eqs. (6) and (7)). Molecular oxygen quenches the excited triplet states in CDOM with similar efficacy, except for very short lived triplet excited states, where the efficacy of quenching by O_2 is reduced. The quantum yield of $^1O_2$ production is thus a convenient indicator of the overall photoreactivity via triplet states of CDOM.

$$\text{CDOM} + h\nu \rightarrow {}^1\text{CDOM}^* \rightarrow {}^3\text{CDOM}^* \quad (6)$$

$${}^3\text{CDOM}^* + O_2 \rightarrow \text{CDOM} + {}^1O_2 \quad (7)$$

Other CDOM photoreactions include the formation of free radicals by homolytic cleavage of bonds or by subsequent chemical reactions following photoionization. Electron paramagnetic resonance can be used to measure some of the free radicals formed during exposure to UV in CDOM from different sources.

We measured singlet oxygen generation and photoproduced free radicals as markers of CDOM photoreactivity. In addition to comparing the photochemical properties of CDOM isolated from zero salinity river water, we used these parameters to track differences in the photoreactivity of CDOM material collected at different points along salinity transects from rivers into the Gulf of Mexico.

4.1. Photophysical characteristics

We found that the ultrafiltration process, which was used to concentrate and isolate CDOM, slightly changes the optical absorption properties in collected samples. Loss of lower molecular mass material corresponds to a disproportionate loss of UV to visible wavelength absorbers as evidenced by a decrease in the slope parameter *S*. A recent work by Mopper et al. (1996) observed similar changes for productive, mid-latitude coastal water, concentrated with Amicon filters as used in the present study. The change in *S* arising in the concentration step, during which lower molecular mass material is lost, can be explained if it is assumed that the CDOM fraction of smaller size absorbs more in the shorter wavelengths (Strome and Miller, 1978; Green and Blough, 1994; Mopper et al., 1996). Although the loss of small molecular mass chromophores may have only a small effect on the photochemical characteristics of the bulk CDOM, we should consider the possible impact when interpreting any results that vary with molecular mass.

The photosensitizing ability of the CDOM was measured by direct detection of $^1O_2$ phosphorescence generated from UV exposure. To our knowledge, this is the first report of direct measurement of $^1O_2$ phosphorescence in natural aquatic CDOM samples.

Previously reported ϕ_{so} values were obtained for natural waters using 2,5-dimethylfuran or furfuryl alcohol as a singlet oxygen scavenger, and fall in the range 0.004–0.030 (Zepp et al., 1977; Haag et al., 1984; Zepp et al., 1985; Frimmel et al., 1987). Our ϕ_{so} values from the HMM samples, obtained from measuring $^1O_2$ phosphorescence directly, fall near the center of this range (Fig. 8). It should be noted that the literature ϕ_{so}'s in Fig. 8 were found using single wavelength excitation of 313 nm or 366 nm. Our excitation light covered the range of 280–380 nm, which included both of the strong Hg lamp lines at 313 nm and 366 nm. Thus our ϕ_{so}'s can be considered average quantum yields for these two lines, and it is reasonable that our ϕ_{so} values should generally fall between the literature values for these two wavelengths.

For our LMM samples, the ϕ_{so} values exceed previously reported values, with the Mississippi River

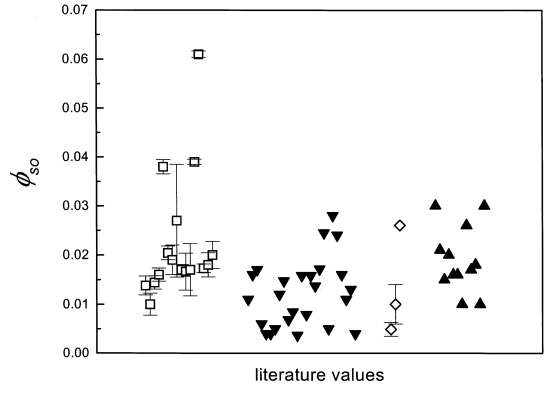

Fig. 8. Comparison of singlet oxygen quantum yields: (□) CDOM concentrated from natural waters, excitation 280–380 nm (this report); (▼) CDOM in natural waters, excitation 313 nm or 366 nm (Zepp et al., 1977, 1985); (◇) humic acids and CDOM concentrated from lake water, excitation 366 nm (Haag et al., 1984); (▲) CDOM extracted from natural waters and soils by XAD-2 resins, excitation 366 nm (Frimmel et al., 1987).

LMM sample having a ϕ_{so} more than twice the highest reported value of 0.03. The large difference between ϕ_{so} values from LMM and HMM fractions indicates that the smaller molecular mass material has higher photosensitizing power. In earlier work on humic and fulvic acids, Frimmel et al. (1987) report a significantly higher sensitizing effect in lower molecular mass fractions. Haag and Hoigné (1986) found that low molecular mass material (range 100–500 Da) from lakes seemed to be more efficient in forming $^1O_2$. In another study, Bruccoleri et al. (1993) measured the triplet state of fulvic acids directly by time resolved photoacoustic spectroscopy. They compared >30 and >1 kDa fractions of Laurentian fulvic acids and found apparent triplet state quantum yields to be much higher for the lower molecular mass fraction. In the smaller CDOM, excited triplet-state chromophores may be less quenched by other components in CDOM, and at the same time may be more accessible for approach and quenching by dissolved molecular oxygen, resulting in higher ϕ_{so}'s. Since low molecular mass CDOM appears to be more efficient in photosensitizing $^1O_2$, and because our optical absorption results indicate that the loss of small material during the process of ultrafiltration changes the distribution of absorbers, our measured $^1O_2$ quantum yields may represent a lower bound for in situ CDOM.

Among the HMM zero salinity samples from the rivers (excluding the partially soluble Blackwater River sample), the singlet oxygen quantum yield varies only slightly. The yield from the Apalachicola was slightly lower than the Mississippi and Atchafalaya River samples, but within the accuracy of this measurement we cannot distinguish between different riverine sources of the CDOM.

Singlet oxygen can also be quenched by the CDOM itself. We have directly observed this quenching and shown that it depends on the concentration of the CDOM (Fig. 4). Although our method does not allow separation of physical from chemical quenching, any chemical quenching will oxidize the CDOM.

We have also measured the steady-state level of photoproducted free radicals in CDOM using EPR. A single EPR line arising from free radicals was readily observed during irradiation. Because we used steady-state EPR, the observed signal must be due to relatively long-lived radicals. Similar spectra with g value ranging from 2.0038 to 2.008 have been reported for humic acids, fulvic acids, particulate organic matter and for soil derived humic substances and are associated with quinone, semiquinone, or substituted semiquinone radical species (Haworth, 1971; Senesi and Schnitzer, 1977; Boughriet et al., 1992; Tipikin et al., 1993). Our measured linewidth in solution indicates an averaging of contributions from several unresolved species of semiquinone radicals (Boughriet et al., 1992). The radicals are produced only during irradiation of the CDOM, and are the result of either direct photolysis or subsequent radical chemistry following photoionization or photosensitized formation of radical pairs. Because these radicals are long-lived, they do not recombine immediately, but are available for other reactions such as oxidation by O_2. Although our experimental conditions are not the same as normally encountered in the environment, if solar UV produces similar radicals to those we observed, this free radical mediated pathway may be an important mechanism for oxidative degradation of DOM.

In contrast to the singlet oxygen generation data, the contribution of small molecular mass constituents does not appear to play an important role in the F.R.P. level. This is similar to the results obtained by Bruccoleri et al. (1993) for Laurentian fulvic acids, where they found that photoionization was not sensitive to molecular mass. We hypothesize that the larger mass material is more likely to stabilize a free radical, increasing the lifetime and allowing detection by EPR. Location of the observed radicals predominantly in the larger mass material would explain the insensitivity of the F.R.P. to inclusion of lower molecular mass CDOM.

We found the EPR signal decayed with continuous, high intensity, short wavelength irradiation (Fig. 6). The loss of the free radical signal was accompanied by a change in the optical absorption, indicating permanent chemical changes in the sample.

4.2. Transport along salinity transects

For the HMM samples, ϕ_{so} values do not decrease along the transects with increasing salinity of the collection sites. Thus singlet oxygen production remains an important photochemical process as

CDOM moves down the river and mixes into ocean waters. Because the values along the transects changed only a small amount, this could indicate that singlet oxygen production is independent of terrigenous or marine origin of the CDOM. However, it is interesting to note that the optical absorption S values of coastal waters, both from our data and others, tend to increase at higher salinities (Blough et al., 1993; Green and Blough, 1994; Vodacek et al., 1997), indicating a higher percentage of small molecular weight material in the bulk CDOM at the high salinities (Strome and Miller, 1978; Green and Blough, 1994; Mopper et al., 1996). In our samples, low molecular mass material was lost in the ultrafiltration process, especially at higher salinities where increases in S have shown that there is more low molecular mass material to begin with. Because of the molecular size selectivity inherent in the ultrafiltration process and because we found that the ϕ_{so} values were dependent on molecular mass, we might expect to see a greater increase in ϕ_{so} with increasing salinity for in situ CDOM than we found with the HMM material.

The ϕ_{so} values for the two LMM samples did not follow the same trend as the HMM samples, with the inshore sample showing a higher quantum yield than the LMM offshore sample. Unlike the HMM samples, the LMM Gulf of Mexico sample had been desalted by diafiltration. During diafiltration small molecular mass material is lost (Benner, 1991), suggesting that the decrease in the ϕ_{so} for the offshore LMM material could be an artifact of the additional processing.

The free radical signal generated in the CDOM decreased dramatically from freshwater samples to samples from 9 ppt estuarine waters (Fig. 7). A variety of physical, chemical, and biological processes influence the behavior of riverine particulate, collodial and dissolved materials in low salinity estuarine transition zones (Duinker, 1980). The stepwise decrease in F.R.P. indicates a decrease in the ability of the material to form the long-lived radicals, probably semiquinones, observed in our experiments. This decrease in radical formation could be due to a decreased ability to stabilize free radicals, and/or a reduction of average molecular size of the CDOM. The drop in F.R.P. does not follow conservative mixing behavior along the salinity transect, making it unlikely that the change is due solely to the increasing presence of marine CDOM. Part of the change in free radical photoreactivity may arise from the changes in the DOM composition as the terrigenous DOM is exposed to the increasing ionic strength of estuarine waters in 0–10 ppt coastal plumes, and part may result from degradation as the material is exposed to light and bacterial processes. The observation in other studies of optical bleaching and the formation of small molecular mass material from CDOM after UV exposure (Kieber et al., 1990; Mopper et al., 1991) and increased bacterial growth (Moran and Zepp, 1997) support a degradation pathway.

5. Conclusions

The measurement of singlet oxygen quantum yield conveniently approximates the formation of long-lived excited states by multiple chromophores in CDOM. As photoproduced free radicals and singlet oxygen may participate in oxidative degradation of CDOM, ϕ_{so} and F.R.P. are complementary and convenient markers of photoreactivity of CDOM from different sources.

Our EPR results show that some aspects of the photochemical nature of the CDOM changes as the terrestrially derived CDOM reaches ≥ 9 ppt estuarine waters. The change indicates a loss of the reactive chemical groups and may reflect degradation of terrestrial CDOM in low salinity waters. In natural environments, the degradation can occur from primary cleavage by UV light or by secondary cleavage from microbial activity, or more likely by a combination of these processes. In contrast to the decrease in F.R.P. values, $^1O_2$ quantum yields along the transect do not decrease for our HMM samples, but remain constant or even increase slightly with increasing salinity. Our results also show that the singlet oxygen quantum yields depend on the presence of low molecular mass material. These results suggest that the photosensitizing ability (photoreactivity via triplet states) of estuarine CDOM does not decrease as terrestrial CDOM is degraded into smaller molecules in estuarine waters or is mixed with low molecular mass marine CDOM.

Acknowledgements

The authors would like to thank R. Benner for the gift of the two low molecular mass samples and the captain and crew of the OSV *Anderson* for their assistance on the transect cruises. We are especially grateful to N. Blough, C. Kelley, A. Motten, and R. Zepp for helpful discussions of this work and comments on the manuscript. Two of the authors, S.L.S. and J.D.P., acknowledge National Research Council Fellowships for this work while at the US EPA. The use of trade names does not imply endorsement by the US EPA.

References

Benner, R., 1991. Ultrafiltration for the concentration of bacteria, viruses, and dissolved organic matter. In: Hurd, D.C., Spencer, D.W. (Eds.), The Analysis and Characterization of Marine Particles. Geophysical Monograph 63. American Geophysical Union, pp. 181–186.

Benner, R., Pakulski, J.D., McCarthy, M., Hedges, J.J., Hatcher, P.G., 1992. Bulk chemical characteristics of dissolved organic matter in the ocean. Science 255, 1561–1564.

Bertilsson, S., Tranvik, L.J., 1998. Photochemically produced carboxylic acids as substrates for freshwater bacterioplankton. Limnol. Oceanogr. 43 (5), 885–895.

Bilski, P., Chignell, C.F., 1996. Optimization of a pulse laser spectrometer for the measurement of the kinetics of singlet oxygen O_2 ($^1\Delta_g$) decay in solution. J. Biochem. Biophys. Methods 33, 73–80.

Bilski, P., Holt, R.N., Chignell, C.F., 1997. Properties of singlet molecular oxygen O_2 ($^1\Delta_g$) in binary solvent mixtures of different polarity and proticity. J. Photochem. Photobiol., A: Chem. 109, 243–249.

Blough, N.V., 1988. Electron paramagnetic resonance measurements of photochemical radical production in humic substances: 1. Effects of O_2 and charge on radical scavenging by nitroxides. Environ. Sci. Technol. 22, 77–82.

Blough, N.V., 1997. Photochemistry in the sea-surface microlayer. In: Liss, P.S., Duce, R.A. (Eds.), The Sea Surface and Global Change. Cambridge Press, Cambridge, pp. 383–424.

Blough, N. V, Zafiriou, O.C., Bonilla, J., 1993. Optical absorption spectra of waters from the Orinoco River outflow: terrestrial input of colored organic matter to the Carribbean. J. Geophys. Res. 98 (C2), 2271–2278.

Blough, N.V., Zepp, R.G., 1995. Reactive oxygen species in natural waters. In: Foote, C.S., Valentine, J.S., Greenberg, A., Liebman, J.F. (Eds.), Active Oxygen in Chemistry. Chapman and Hall, New York, pp. 280–331.

Boughriet, A., Ouddane, B., Wartel, M., 1992. Electron spin resonance investigations of Mn compounds and free radicals in particles from the Seine river and its estuary. Mar. Chem. 37, 149–169.

Bricaud, A., Morel, A., Prieur, L., 1981. Absorption by dissolved organic matter of the sea (yellow substance) in the UV and visible domains. Limnol. Oceanogr. 26 (1), 43–53.

Bruccoleri, A., Pant, B.C., Sharma, D.K., Langford, C.H., 1993. Evaluation of primary photoproduct quantum yields in fulvic acids. Environ. Sci. Technol. 27, 889–894.

Bushaw, K.L., Zepp, R.G., Tarr, M.A., Schulz-Jander, D., Bourbonniere, R.A., Hodson, R.E., Miller, W.L., Bronk, D.A., Moran, M.A., 1996. Photochemical release of biologically available nitrogen from aquatic dissolved organic matter. Nature 381, 404–407.

Carder, K.L., Steward, R.G., Harvery, G.R., Ortner, P.B., 1989. Marine humic and fulvic acids: their effects on remote sensing of ocean chlorophyll. Limnol. Oceanogr. 34 (1), 68–81.

Chin-Leo, G., Benner, R., 1992. Enhanced bacterioplankton production and respiration at intermediate salinities in the Mississippi River plume. Mar. Ecol. Prog. Ser. 87, 98–102.

Coble, P.G., 1996. Characterization of marine and terrestrial DOM in seawater using excitation–emission matrix spectroscopy. Mar. Chem. 51, 325–346.

Coble, P.G., Brophy, M.M., 1994. Investigation of the geochemistry of dissolved organic matter in coastal waters using optical properties. SPIE, 2258: Ocean Optics, 12, pp. 377–389.

Coble, P.G., Del Castillo, C.E., Avril, B., 1998. Distribution and optical properties of CDOM in the Arabian Sea during the 1995 Southwest Monsoon. Deep-Sea Res. II 45, 2195–2223.

Cooper, W.J., Zika, R.G., Petasne, R.G., Fischer, A.M., 1989. Sunlight-induced photochemistry of humic substances in natural waters: major reactive species. In: Suffet, I.H., MacCarthy, P. (Eds.), ACS Symposium Series 219. American Chemical Society, Washington, DC, pp. 333–362.

Davies-Colley, R.J., Vant, W.N., 1987. Absorption of light by yellow substance in freshwater lakes. Limnol. Oceanogr. 32 (2), 416–425.

Duinker, J.C., 1980. Suspended matter in estuaries: adsorption desorption processes. In: Olausson, E., Cato, I. (Eds.), Chemistry and Biogeochemistry of Estuaries. Wiley, New York, pp. 121–152.

Faust, B.C., Hoigné, J., 1987. Sensitized photooxidation of phenols by fulvic acid and in natural waters. Environ. Sci. Technol. 21, 957–964.

Fischer, A.M., Kliger, D.S., Winterle, J.S., Mill, T., 1985. Direct observation of phototransients in natural waters. Chemosphere 14 (9), 1299–1306.

Frimmel, F.H., Bauer, H., Putzien, J., Murasecco, P., Braun, A.M., 1987. Laser flash photolysis of dissolved aquatic humic material and the sensitized production of singlet oxygen. Environ. Sci. Technol. 21 (6), 541–545.

Gould, I.R., 1989. Conventional light sources. In: Scaiano, J.C. (Ed.), Handbook of Organic Photochemistry, Vol. 1. CRC Press, Boca Raton, FL, pp. 155–196.

Green, S.A., Blough, N.V., 1994. Optical absorption and fluorescence properties of chromophoric dissolved organic matter in natural waters. Limnol. Oceanogr. 39 (8), 1903–1916.

Guo, L., Santschi, P.H., Warnken, K.W., 1995. Dynamics of dissolved organic carbon (DOC) in oceanic environments. Limnol. Oceanogr. 40 (8), 1392–1403.

Haag, W.R., Hoigné, J., 1986. Singlet oxygen in surface waters: 3. Photochemical formation and steady-state concentrations in various types of waters. Environ. Sci. Technol. 20, 341–348.

Haag, W.R., Hoigné, J., Gassman, E., Braun, A.M., 1984. Singlet oxygen in surface waters: Part II. Quantum yields of its production by some natural humic materials as a function of wavelength. Chemosphere 13 (5/6), 641–650.

Haworth, R.D., 1971. The chemical nature of humic acid. Soil Sci. 111 (1), 71–79.

Hedges, J.J., Hatcher, P.G., Ertel, J.R., Meyers-Schulte, K.J., 1992. A comparison of dissolved humic substances from seawater with Amazon counterparts by ^{13}C-NMR spectroscopy. Geochim. Cosmochim. Acta 56, 1753–1757.

Kieber, D.J., Blough, N.V., 1990. Determination of carbon-centered radicals in aqueous solution by liquid chromatography with fluorescence detection. Anal. Chem. 62 (21), 2275–2283.

Kieber, R.J., Zhou, X., Mopper, K., 1990. Formation of carbonyl compounds from UV-induced photodegradation of humic substances in natural waters: fate of riverine carbon in the sea. Limnol. Oceanogr. 35 (7), 1503–1515.

Mantoura, R.F.C., Woodward, E.M.S., 1983. Conservative behavior of riverine dissolved organic carbon in the Severn estuary: chemical and geochemical implications. Geochim. Cosmochim. Acta 47, 1293–1309.

Miller, W.L., Moran, M.A., 1997. Interaction of photochemical and microbial processes in the degradation of refractory dissolved organic matter from a coastal marine environment. Limnol. Oceanogr. 42 (6), 1317–1324.

Miller, W.L., Zepp, R.G., 1995. Photochemical production of dissolved inorganic carbon from terrestrial input: significance to the oceanic organic carbon cycle. Geophys. Res. Lett. 22, 417–420.

Mopper, K., Zhiming, F., Bentjen, S.B., Chen, R.F., 1996. Effects of cross-flow filtration on the absorption and fluorescence properties of seawater. Mar. Chem. 55, 53–74.

Mopper, K., Zhou, X., 1990. Hydroxyl radical photoproduction in the sea and its potential impact on marine processes. Science 250, 661–664.

Mopper, K., Zhou, X., Kieber, R.J., Kieber, D.J., Sikorski, R.J., Jones, R.D., 1991. Photochemical degradation of dissolved organic carbon and its impact on the oceanic carbon cycle. Nature 353, 60–62.

Moran, M.A., Pomeroy, L.R., Sheppard, E.S., Atkinson, L.P., Hodson, R.E., 1991. Distribution of terrestrially derived dissolved organic matter on the southeastern U.S. continental shelf. Limnol. Oceanogr. 36, 1134–1149.

Moran, M.A., Zepp, R.G., 1997. Role of photoreactions in the formation of biologically labile compounds from dissolved organic matter. Limnol. Oceanogr. 42 (6), 1307–1316.

Opsahl, S., Benner, R., 1997. Distribution and cycling of terrigenous dissolved organic matter in the ocean. Nature 386, 480–482.

Petasne, R.G., Zika, R.G., 1987. Fate of superoxide in coastal sea water. Nature 325, 516–518.

Schmidt, R., Tanielian, C., Dunsbach, R., Wolff, C.J., 1994. Phenalenone, a universal reference compound for the determination of quantum yields of singlet oxygen O_2 (Δ_g^1) sensitization. J. Photochem. Photobiol., A: Chem. 79, 11–17.

Senesi, N., Schnitzer, M., 1977. Effects of pH, reaction time, chemical reduction and irradiation on ESR spectra of fulvic acid. Soil Sci. 123 (4), 224–234.

Strome, D.J., Miller, M.C., 1978. Photolytic changes in dissolved humic substances. Verh. Int. Verein. Limnol. 20, 1248–1254.

Stumm, W., Morgan, J.J., 1996. Aquatic Chemistry: Chemical Equilibria and Rates in Natural Waters, 3rd edn. Wiley, New York, pp. 726–759.

Tipikin, D.S., Lazarev, G.G., Zhorin, V.A., Lebedev, Ya.S., 1993. An EPR and mechanical activation study of the nature of stable radicals in humic acids. Russian J. Phys. Chem. 67 (9), 1646–1650.

Vaughan, P.P., Blough, N.V., 1998. Photochemical formation of hydroxyl radical by constituents of natural waters. Environ. Sci. Technol. 32, 2947–2953.

Vodacek, A., Blough, N.V., DeGrandpre, M.D., Peltzer, E.T., Nelson, R.K., 1997. Seasonal variation of CDOM and DOC in the Middle Atlantic Bight: terrestrial inputs and photooxidation. Limnol. Oceanogr. 42 (4), 674–686.

Wetzel, R.G., Hatcher, P.G., Bianchi, T.S., 1995. Natural photolysis by ultraviolet irradiance of recalcitrant dissolved organic matter to simple substrates for rapid bacterial metabolism. Limnol. Oceanogr. 40 (8), 1369–1380.

Yentsch, C.S., Reichert, C.A., 1962. The interrelationship between water-soluble yellow substances and chloroplastic pigments in marine algae. Bot. Mar. 3, 65–74.

Zafiriou, O.C., 1974. Sources and reactions of OH and daughter radicals in seawater. J. Geophys. Res. 79, 4491–4497.

Zafiriou, O.C., 1990. Chemistry of superoxide ion-radical (O_2^-) in seawater: I. pK^*_{asw} (HOO) and uncatalyzed dismutation kinetics studies by pulse radiolysis. Mar. Chem. 30, 31–43.

Zepp, R.G., Schlotzhauer, P.F., 1981. Comparison of photochemical behavior of various humic substances in water: III. Spectroscopic properties of humic substances. Chemosphere 10 (5), 479–486.

Zepp, R.G., Schlotzhauer, P.F., Sink, R.M., 1985. Photosensitized transformations involving electronic energy transfer in natural waters: Role of humic substances. Environ. Sci. Technol. 19 (1), 74–81.

Zepp, R.G., Wolfe, N.L., Baughman, G.L., Hollis, R.C., 1977. Singlet oxygen in natural waters. Nature 267 (5610), 421–423.